DEUTSCHES ELEKTRONEN-SYNCHROTRON DESY

DESY SR 83-13
August 1983

Eigentum der DESY Bibliothek
Property of DESY library
Zugang: 26. SEP. 1983
Accessions:
Leihfrist: 7 Tage
Loan period: 7 days

MEASUREMENT OF THE POLARIZATION OF X-RAYS FROM A SYNCHROTRON SOURCE

by

G. Materlik

Hamburger Synchrotronstrahlungslabor HASYLAB at DESY

P. Suortti

Department of Physics, University of Helsinki, Helsinki

ISSN 0723-7979

NOTKESTRASSE 85 · 2 HAMBURG 52

DESY behält sich alle Rechte für den Fall der Schutzrechtserteilung und für die wirtschaftliche
Verwertung der in diesem Bericht enthaltenen Informationen vor.

DESY reserves all rights for commercial use of information included in this report, especially in
case of filing application for or grant of patents.

To be sure that your preprints are promptly included in the
HIGH ENERGY PHYSICS INDEX ,
send them to the following address (if possible by air mail) :

DESY
Bibliothek
Notkestrasse 85
2 Hamburg 52
Germany

DESY SR 83-13
August 1983

MEASUREMENT OF THE POLARIZATION OF X-RAYS FROM
A SYNCHROTRON SOURCE

G. Materlik, Hamburger Synchrotronstrahlungslabor HASYLAB,
Deutsches Elektronen-Synchrotron DESY, Notkestrasse 85,
D-2000 Hamburg 52, Germany (FRG)

and

P. Suortti, Department of Physics, University of Helsinki,
Siltavuorenpenger 20 D, 00170 Helsinki 17, Finland

ISSN 0723-7979

to be published in: Journal of Applied Crystallography

Abstract

The vertical intensity distributions of x-rays from a synchrotron source are measured by powder diffraction. The components polarized in the orbital plane and perpendicular to this plane are separated by measuring a reflection 90° to the vertical and horizontal plane, respectively. The measurements are made at three wavelengths between $0.65\lambda_c$ and λ_c, where λ_c is the characteristic wavelength. In each case, the degree of linear polarization reaches a maximum of 90 % at the center of the beam. The results agree closely with calculations which use machine optical parameters.

1. Introduction

The state of polarization of x-rays enters the scattering cross-section, and has to be determined by an independent measurement or calculation. This situation was recognized in very early experiments with conventional x-ray sources, where the beam was monochromatized typically by a mosaic crystal. The spectral distribution of synchrotron radiation can be reliably calculated from the theory, and most workers have accepted the ideal picture where the beam is perfectly polarized in the orbital plane and elliptically outside. However, the ideal distribution must be convoluted by the source size and source divergences (Materlik & Kostroun, 1980) and the focusing functions of the beam optics. These can be included in a ray-tracing calculation, but this assumes ideal surfaces of the optical elements, and in practice the beam will be blurred by uncontrollable irregularities of the surfaces. The ray-tracing calculations give invaluable guidelines for construction of the optical system, but they are not substitutes for actual beam diagnostics.

Early measurements of the polarization of x-rays from a synchrotron (SXR) found a good qualitative agreement between theory and experiment (Bathow, Freytag & Haensel, 1966). Recent attempts (Materlik & Rohloff, 1980; Phillips, Wladower & Hodgson, 1976; Brunel, Patrat, de Bergevin, Rousseaux & Lemonnier, 1982) to determine the degree of polarization of SXR from storage rings reveal that the degree of polarization can approach the average polarization even in the orbital

plane. It is obvious that the degree of polarization is a parameter which must be measured for each experimental setting. The purpose of this note is to describe a simple and fast method for determining this parameter.

2. Intensity and Polarization

The relevant variables in a diffraction measurement with SXR are best illustrated with a phase-space diagram. Fig. 1 shows the vertical distributions with no focussing elements in the beam line. The equi-intensity contours are due to the finite height of the electron beam and convolution of the electron beam divergences with the radiation distributions, which are denoted by $P_{r,\parallel}$ (electric vector parallel to the orbital plane) and $P_{r,\perp}$ (electric vector perpendicular to the orbital plane). The resolution of the diffraction measurement is determined by the active area and angular reflection range of the sample, as indicated by the shaded area in Fig. 1. The degree of linear polarization is a function of position y and divergence y', $K(y,y') = (I_{\parallel} - I_{\perp})/(I_{\parallel} + I_{\perp})$. The integrated intensity of a reflection, which is of primary interest in most x-ray diffraction experiments, is found by scanning along y', and the appropriate K is the corresponding average K(y), as shown in Fig. 1. Various possibilities of measuring K(y) will be considered in the following.

The scattering cross-section of x-rays can be written as (Suortti, 1979)

$$\frac{d^2\sigma}{d\omega_2 d\Omega} = r_e^2 \frac{\omega_2}{\omega_1} (\hat{e}_1 \cdot \hat{e}_2)^2 \sum_A \sum_B |\langle B|e^{i\underline{k}\cdot\underline{r}}|A\rangle|^2 \delta(E_B - E_A - \hbar\omega) \quad (1)$$

+ resonant scattering
+ multiple scattering.

Here $r_e = e^2/mc^2$ is the classical electron radius, ω_1 the angular frequency of the incident radiation and ω_2 that of the scattered radiation, $\hat{e}_1$ and $\hat{e}_2$ the respective (unit) vectors of the electric fields, A the initial and B the final state with energies E_A and E_B, respectively, $\underline{k} = \underline{k}_1 - \underline{k}_2$ the scattering vector, and $\omega = \omega_1 - \omega_2$. The first term of non-resonant scattering includes all processes where the total number of photons remains unchanged. In a solid the correlations of atomic positions and interactions between atoms brake this into elastic Bragg scattering from the average structure, and inelastic scattering where various excitations of the solid are involved, such as phonons, plasmons and electrons. The resonant part includes fluorescence, resonant Raman scattering, and possibly scattering via impurity states. In the present context, the essential difference is that the non-resonant part includes the polarization factor $\hat{e}_1 \cdot \hat{e}_2$, while the resonant scattering may exhibit only insignificant polarization dependence through coupling of the final and initial states. Multiple processes of any combination of the components of the non-resonant part may change substantially the state of polarization of the total non-resonant scattering, if the cross-sections and the path lengths in the sample before photon annihilation or escape are large enough.

From the expression for the single non-resonant scattering in Eq. 1 and from Fig. 2 we see that at the scattering angle of 90° the scattering power is proportional to $|e_{1\sigma}|^2$, and only the electric vector perpendicular to the plane of scattering contributes to the power. In the case of SXR, the component parallel to the orbit plane, $P_{\parallel}$, is observed when the plane of scattering is vertical and the perpendicular component, $P_{\perp}$, in the orbit plane.

In order to be able to separate properly the two components of polarization by an intensity measurement, a few requirements must be satisfied: (i) geometrical conditions are well defined and the same in both measurements, (ii) single non-resonant scattering must be of sufficient intensity and easily separable from multiple and resonant scattering.

It has been demonstrated that the polarization ratio can be determined even at the level of 10^{-5} when a multiple reflection arrangement is employed (Hart & Rodriguez, 1979). In cases where an accuracy of the order of 10^{-3} is sufficient several other methods can be used. The best ratio of single non-resonant scatteringto the background is obtained in a $2\theta = 90^o$ Bragg reflection from a perfect crystal. This measurement requires a precise angular scan over the reflection. Another possibility is to utilize anomalous transmission or the Borrmann effect. If a thick perfect crystal is reflecting in the Laue case, it is found that excited wave fields with the electric vector parallel to the Bragg planes are transmitted through the crystal with very little absorption, while those with the electric vector parallel to the plane

of reflection are extinguished. The roles of the components are interchanged by rotating the crystal by 90° about the beam direction (Cole, Chambers & Wood, 1961). With a suitable selection of crystals, this method easily covers a large wavelength range, but again for each measurement an angular scan must be performed. Note, however, that perfect crystal arrangements exhibit an extremely unsymmetric angular acceptance and emittance in the reflection plane and perpendicular to such plane. When perfect crystal polarimeters are used, the determination of the polarisation degree always has to take these geometrical factors (as well as source unisotropies) very carefully into account.

As to the signal-to-noise ratio, the next best choice is a powder sample with strong, separable reflection near $2\theta = 90^{\circ}$. This is a relatively easy requirement to satisfy, as suitable materials are abundant. No scan is needed for an integration over y', if a wide enough receiving slit is used. The most straightforward choice would be an amorphous sample that gives sufficient diffuse scattering at $2\theta = 90^{\circ}$, but here single non-resonant scattering may be too small in comparison with the background of multiple and resonant scattering. In the following we are going to look to this situation in detail.

3. Amorphous and Powder Samples

A thorough treatment of non-resonant scattering from an

amorphous sample is given by Warren (1969). At large enough values of the scattering vector the interference effects can be ignored in estimates of intensity, and the flux of scattered photons is

$$n(2\theta) = n_o \Omega r_e^2 N J(2\theta) K_{pol} \int_0^T \exp(-2\mu z/\sin\theta) \frac{dz}{\sin\theta} , \qquad (2)$$

where n_o is the incident flux, Ω the solid angle , N the number of scattering units per unit volume, $J(2\theta)$ the corresponding cross-section given in electron units, in the present case the polarization factor K_{pol} is unity, and for a totally absorbing sample in symmetrical reflection the value of the integral is $1/2\mu$, where μ is the linear absorption coefficient.

The ratio of double scattering to single scattering from an amorphous sample is of the following form (Warren, 1969),

$$\frac{n(2)}{n(1)} = \frac{N}{J(2\theta)\mu} \int_{-\pi}^{\pi} \int_{-\pi/2}^{\pi/2} \frac{J(2\theta_1)J(2\theta_2)}{A(\theta,\epsilon)} \; K_{pol}(\theta_1,\theta_2) \, d\epsilon d\varphi . \quad (3)$$

There is a simple geometrical relationship between the successive scattering angles (θ_1,θ_2) and θ,ϵ,φ. $A(\theta,\epsilon)$ is an angular factor. Some values for vitreous SiO_2 are included in Table 1, and these indicate that $n(2)/n(1)$ becomes intolerably large at short wavelengths; other choices of the scatterer do not improve the situation essentially.

The photon flux of a symmetrical reflection from a totally

absorbing powder sample is (Suortti & Jennings, 1977)

$$n_{hkl} = n_o r_e^2 N^2 \psi K_{pol} \frac{\lambda^3 p_{hkl}}{16\pi\mu \sin\theta} \frac{F_{hkl}^2}{\sin 2\theta} , \qquad (4)$$

where ψ is the planar angle intercepted by the slit height h, i.e. $\psi \simeq h/R$, where R is the distance of the slit from the sample , p_{hkl} is the multiplicity, and F the structure factor of a unit cell of volume 1/N.

A few calculated values of n_{hkl} are given in Table 1. The input data are taken from various measurements and tabulated values (International Tables for X-ray Crystallography, 1962, 1974; Merisalo & Inkinen, 1966; Suortti & Jennings, 1977). The surprising fact is that at short wavelenths there is more scattering from an amorphous sample to a slit of size $(h/R)^2 = 5 \cdot 10^{-3}$ than from a powder reflection to a slit of the same height. The explanation is simple: total scattering from a powder sample is approximately the same as that from an amorphous sample of the same compound, and when the angular spacing of the reflections becomes smaller than the width of the slit, w/R (= h/R here), scattering to one reflection is less than the average scattering to the slit. The advantage of using a powder sample is that the Bragg reflection can be separated from the background, and only a relatively narrow slit is required to compass most of the reflection; typically $w \simeq h/10$ would be sufficient, and this would reduce multiple and resonant scattering by a factor of 10. When the wavelength increases the powder scattering is concentra-

ted to fewer reflections, and the observed intensity becomes much larger than that from an amorphous sample.

4. Measurements

The measurements were made on the beam of the ROEMO station at HASYLAB (DESY, Hamburg). The electron energy of the storage ring DORIS was 3.3 GeV, and the characteristic wavelength 1.9 Å (6.6 keV). The vertical height of the electron beam as given by the beam optic parameters was 1.25 mm (FWHM) with a source divergence 0.14 mrad (FWHM). The experiment was located 35 m from the source, and no focussing elements were used in the SXR beam. The monochromator was built as a pair of symmetrically reflecting Si (111) crystals in the parallel (1,-1) setting. The intensity of the SXR beam was of the order of 10^7 c/s/mm^2 when the electron current was 50 mA, and there was a small wavelength gradient in the vertical direction.

The construction of the polarizer is shown in Fig. 3. The components are attached to a tube which is aligned parallel to the SXR beam and can be rotated about the beam. The powder sample is spun about the surface normal. The receiving slit and the detector are attached to a cross-bar which can be moved by a small synchronous motor to scan a 4° angular region on both sides of $2\theta = 90^o$. The motor is operated via remote control, and the position of the receiving assembly is read from the output voltage of a

potentiometer which is coupled to the linear drive of the cross-bar; the input voltage is regulated by a Zener diode.

The wavelength of the SXR beam was selected to exite a strong reflection from the Mo powder sample near $2\theta = 90^{o}$. The location and profile of the reflection was studied by scanning with a narrow receiving slit. The width of the reflection was almost entirely due to the circular collimator in front of the sample (diameter 1.3 mm), and a slit of $\Delta(2\theta) = 1.2^{o}$ was found sufficient to compass the powder reflection. Background was measured on both sides of the reflection and was subtracted from the integrated reflection. Background scattering of the proper wavelength was very small, but the $\lambda/3$ harmonic from the monochromator excited MoK fluorescence, which could only be partially removed by pulse height discrimination of the NaI(Tl) output. On the other hand, estimates from Eq. 4 show that the high energy harmonics have negligible effects on the Bragg reflections. When the scattering angle is $2\theta = 90^{o} \pm \vartheta$, there is a contribution $P_{\pi}\sin^{2}\vartheta$ from the component which has the electric vector in the plane of scattering. If a 0.1 % contamination is tolerated, $\vartheta \leq 2^{o}$.

The polarizer was mounted on a table with remotely controlled height, so that the vertical intensity distributions could be scanned by recording the integrated intensity of the powder reflection on paper chart as a function of table height; similar scans were made of the background. The intensity of the incident beam was monitored with an ionization chamber in order to make various measurements comparable. The intensity estimates of Table 1 indicate close agreement between the calculated and measured absolute values.

5. Results and Discussion

The results of the measurements at three wavelengths are summarized in Fig. 4. The radiation is not even at the center of the beam linearly polarized, but there is 5 % contribution of the perpendicular component. The situation is much the same in all three cases, as the wavelength varies only from $0.65\lambda_{c}$ to λ_{c}. The edges of the monochromator limit the distributions at the shortest wavelength, but otherwise the SXR beam optic does not change the intensity distributions except by the polarization factor of the double monochromator, which is 1 for the parallel and $\cos^{2}2\theta_{M}$ for the perpendicular component. Therefore the smearing of the intensity distributions is due to the vertical dimension and divergence of the effective source. The calculated distributions, which are based on the parameters of the machine optic of DORIS[+], agree very closely with the measurement, as seen in Fig. 5. An approximate analytical integration of the phase-space diagram of Fig. 1 gives results which are almost identical with the

[+]A general computer program for this calculation was developed at HASYLAB by B. Schönfeld and G. Tolkiehn.

numerical integration of the actual theoretical bivariate distributions. The working formulas for the approximate calculation are given in the Appendix.

Focussing optic typically mixes the two components of polarization. This can be included in ray-tracing calculation, but the smearing due to surface irregularities makes the result questionable. The intensity distributions of the two components should be measured, and the present results show that this can be done fast and reliably by powder diffraction. The limiting factor is the integrated intensity of the powder reflection, but typically sufficient flux (10^7 to 10^8 photons/sec) is passed by a collimator which is small in comparison with the cross-section of the beam. Practical considerations determine the choice of the powder sample: the reflections to be used should be strong andeasily separable and the background level should be low. If 0.5 % scattering from the major parallel component is allowed in the measurement of the perpendicular component, the scattering angle can be between 86° and 94°. Table 2 demonstrates that within these limits, wide wavelength ranges can be covered with <u>one</u> powder sample.

If the polarisation ratio is to be known at the level of 10^{-3}, a 90° reflection from a perfect crystal or a Borrmann polarizer is recommended, and at short wavelengths these may be the only feasible choices at any account. The scan which is required for an integration over the wavelength and divergence distributions may be effected by oscillating

the crystal about the reflecting position, and this can be realized by a simple device (Chandrasekhar, Ramaseshan & Singh, 1969).

The lack of perfect polarization of the SXR beam has various effects in experiments. Typically in a measurement with SXR the plane of diffraction is vertical, and the relative contribution of the perpendicular component decreases from $I_\perp/(I_\parallel + I_\perp)$ to zero when the scattering angle 2θ changes from 0 to 90°. The effects of the perpendicular component may be disastrous in a measurement of weak resonant scattering in the horizontal plane at $2\theta = 90^\circ$, if the non-resonant scattering is assumed to be zero. Also a general comment is due. The measurements which are described in this paper do not necessarily yield the complete information about the state of polarization. For instance, the results are identical for circularly polarized and unpolarized beams. The degree of circular polarization must be known in studies of magnetic distributions, and it has been demonstrated that it can be determined from the magnetic scattering of a sample of known magnetization (Brunel et al., 1982).

We thank B. Schönfeld for his support in calculating the synchrotron radiation spectrum including the machine optic.

Appendix

The vertical distributions of the radiation from one electron, as illustrated in Fig. 6, may be approximated by

$$P_{r,\parallel}(y') \simeq \exp(-y'^2/2\sigma_\parallel'^2) \quad \text{(A.1a)}$$

$$P_{r,\perp}(y') \simeq a\{\exp[-(y'-y_0')^2/2\sigma_\perp'^2]+\exp[-(y'+y_0')^2/2\sigma_\perp'^2]\}. \quad \text{(A.1b)}$$

These distributions are convoluted by the size and divergence distributions of the electron beam segment seen by the experiment. These can be approximated by

$$P_e(y,y') \simeq \exp(-y^2/2\sigma_e^2 - y'^2/2\sigma_e'^2) \quad \text{(A.2)}$$

The equi-intensity contours of the source distributions are illustrated in Fig. 1a, and the distributions at distance D from the source are obtained when y is replaced by y-y'D in the convolutions

$$P_\parallel = P_{r,\parallel}(y')*P_e(y,y') \quad \text{(A.3a)}$$

$$P_\perp = P_{r,\perp}(y')*P_e(Y,y') \quad \text{(A.3b)}$$

Reflection from a powder sample integrates over y' (see Fig. 1b), and the intensity distributions are

$$I_\parallel(y) \simeq \exp(-y^2/2\Sigma_\parallel^2) \quad \text{(A.4a)}$$

$$I_\perp(y) \simeq b\exp[-(y^2+D^2y_0'^2)/2\Sigma_\perp^2]\cosh(Dy_0'y/\Sigma_\perp^2) \quad \text{(A.4b)}$$

where $\Sigma_\parallel^2 = \sigma_e^2 + D^2(\sigma_e'^2 + \sigma_\parallel'^2)$ and a similar expression holds for $\Sigma_\perp^2$. The scaling constant b is determined from

$$b = \frac{p_\perp}{1-p_\perp} \frac{(\sigma_e'^2 + \sigma_\parallel'^2)^{\frac{1}{2}}}{(\sigma_e'^2 + \sigma_\perp'^2)^{\frac{1}{2}}} , \quad \text{(A.5)}$$

where $p_\perp$ is the total fraction of the perpendicular component. In addition, $I_\parallel(y)$ and $I_\perp(y)$ must be multiplied by the polarization factors of the monochromator.

References

Bathow, G., Freytag, E. & Haensel, R. (1966). J. Appl. Phys. 37, 3449-3454.

Brunel, M., Patrat, G., de Bergevin, F., Rousseaux, F. & Lomonnier, M. (1982). Acta Cryst. A39, 84-88.

Chandrasekhar, S., Ramaseshan, S. & Singh, A.K. (1969). Acta Cryst. A25, 140-142.

Cole, H., Chambers, F.W. & Wood, C.G. (1961). J. Appl. Phys. 32, 1942-1945.

Green, G.K. (1977). Brookhaven National Laboratory Publ. 50595, Vol. II, 1-90.

Hart, M. & Rodriguez, A.R.D. (1979). Phil. Mag. B40, 149-157.

International Tables for X-ray Crystallography, Vol. III (1962), Vol. IV (1974). Birmingham, Kynoch Press.

Materlik, G. & Kostroun, V.O. (1980). Rev. Sci. Instrum. 51, 86-94.

Materlik, G. & Rohloff, K.-B. (1980). HASYLAB Jahresbericht, 134.

Merisalo, M. & Inkinen, O. (1966). Ann. Acad. Sci. Fenn. A VI, 207.

Phillips, J.C., Wladower, A. & Hodgson, K.O. (1976). Stanford Synchrotron Radiation Laboratory Report 76/01.

Suortti, P. (1979). Phys. stat. solidi (b) 91, 657-666.

Suortti, P. & Jennings, L.D. (1977). Acta Cryst. A33, 1012-1027.

Warren, B.E. (1969). "X-ray Diffraction", Reading, Mass., Addison-Wesley.

Table 1. Calculated and measured values of the integrated intensity of powder reflections and amorphous scattering from totally absorbing samples at $2\theta = 90^{\circ}$. The slit height $h/R = 8.73 \cdot 10^{-2}$ and the solid angle $\Omega = 7.6 \cdot 10^{-3}$ correspond to a maximum deviation of $\pm 2.5^{\circ}$ from the 90° reflection.

λ/Å		2θ	p_{hkl}	$J(2\theta)$, $f^2 e^{-2M}$	μ/cm^{-1}	$N/cm^3/10^{22}$	n(2)/n(1)	$(n/n_o)\cdot 10^5$	$(n/n_o)\cdot 10^5$
0.615	Vitr. SiO_2	90		8.1	5.45	2.21	0.08	0.98	
	LiF (753,911)	88.1	72	0.258	2.51	6.12		0.25	
	LiF (842)	88.8	48	0.373					
1.000	Vitr. SiO_2	90		25.3	21.7		0.03	0.90	
	Mo(420)	90.8	24	195	495	6.42		0.75	
1.542	Vitr. SiO_2	90		57.8	75.8		0.01	0.59	
	Cu(311)	90.2	24	131	472	8.46		3.42	
								(calc)	(meas)
1.20	Mo(321)							2.66	2.75
1.60	Mo(220)							1.05	1.30
1.85	Mo(211)							2.61	2.84

Table 2. Reflections from a powder sample of bcc Mo. For $86^\circ \leq 2\theta \leq 94^\circ$ less than 0.5 % of the polarization component with the electric vector in the plane of diffraction is reflected, and λ_{min} to λ_{max} gives the corresponding wavelength span. The slit height is the same as in Table 1, $h/R = 8.73 \cdot 10^{-2}$.

hkl	λ_{min}/Å	λ_{max}/Å	$(n/n_o) \cdot 10^5$
321	1.145	1.228	2.66
400	1.071	1.148	0.30
330,411	1.010	1.083	1.62
420	0.958	1.027	0.97
332	0.913	0.979	0.88
422	0.874	0.938	0.80
510,431	0.840	0.901	2.20
521	0.782	0.839	1.23
530,433	0.735	0.787	1.03

Figure captions

Fig. 1. Phase-space diagrams of the vertical distribution of SXR. At the center of the source, a) shows the 1σ-contour for the electron beam (dotted curve) and the contours of the convoluted radiation distributions (solid curve for the parallel component, dashed curve for the perpendicular one). The radiation distributions at distance D from the source are shown in b); the shaded area indicates reflection by a small single crystal, and the arrow an angular scan.

Fig. 2. 90° scattering of synchrotron radiation. The polarization vector of the incident radiation, e_1, is divided into components perpendicular to the plane of scattering, $e_{1\sigma}$, and parallel to this plane, $e_{1\pi}$. The incident power P is divided into two components, $P_{\parallel}$ and $P_{\perp}$, which are proportional to $e_{1\parallel}^2$ and $e_{1\perp}^2$, respectively.

Fig. 3. Powder reflection polarizer. The structures are attached to a tube whose axis is aligned parallel to the incident beam. Circular collimators coincide with the axis. The powder sample (PS) is mounted on a small goniometer head, where it can be set at the calculated scattering angle and spun about the surface normal. The receiving slit assembly (RS) and the dedector (D) are attached to a cross-bar which can be driven perpendicularly to the reflected beam. This drive (M) is coupled to a linear potentiometer (P), which is used for indication of

Figure captions (cont.)

the position of the receiving assembly.

Fig. 4. The degree of perpendicular and linear polarization as a function of the vertical distance from the center of the beam at distance D = 35 m from the source. At λ = 1.20 Å the beam was cut by the edges of the monochromator (dotted curve); the other wavelengths are 1.60 Å (dashed curve) and 1.85 Å (solid curve). $K_\perp = I_\perp/(I_\parallel + I_\perp)$, $K = (I_\parallel - I_\perp)/(I_\parallel + I_\perp)$

Fig. 5. Experimental and calculated vertical intensity distributions at D = 35 m, when λ = 1.85 Å. The solid curves are obtained by a numerical integration of the SXR distributions (Green, 1977), and the dashed curves are from an approximate calculation with the same machine optic parameters σ_e = 0.53 mm and $\sigma'_e = 0.60 \cdot 10^{-4}$ (see Appendix). The experimental points are for the parallel component (circles) and the perpendicular component (crosses); the arrow indicates the cut-off by the edge of the monochromator.

Fig. 6. Divergence distributions of the SXR from one electron at $\lambda = \lambda_c$ (Green, 1977). The angle with the electron trajectory is denoted by Ψ, and $\gamma = E/E_o$ = 3300 MeV/0.511 MeV = 6460 in the present case. With these values, the variances of the distributions are $\sigma'_\parallel = 0.88 \cdot 10^{-4}$ and $\sigma'_\perp = 0.486 \cdot 10^{-4}$, and the perpendicular distribution peaks at $y'_o = 1.10 \cdot 10^{-4}$.

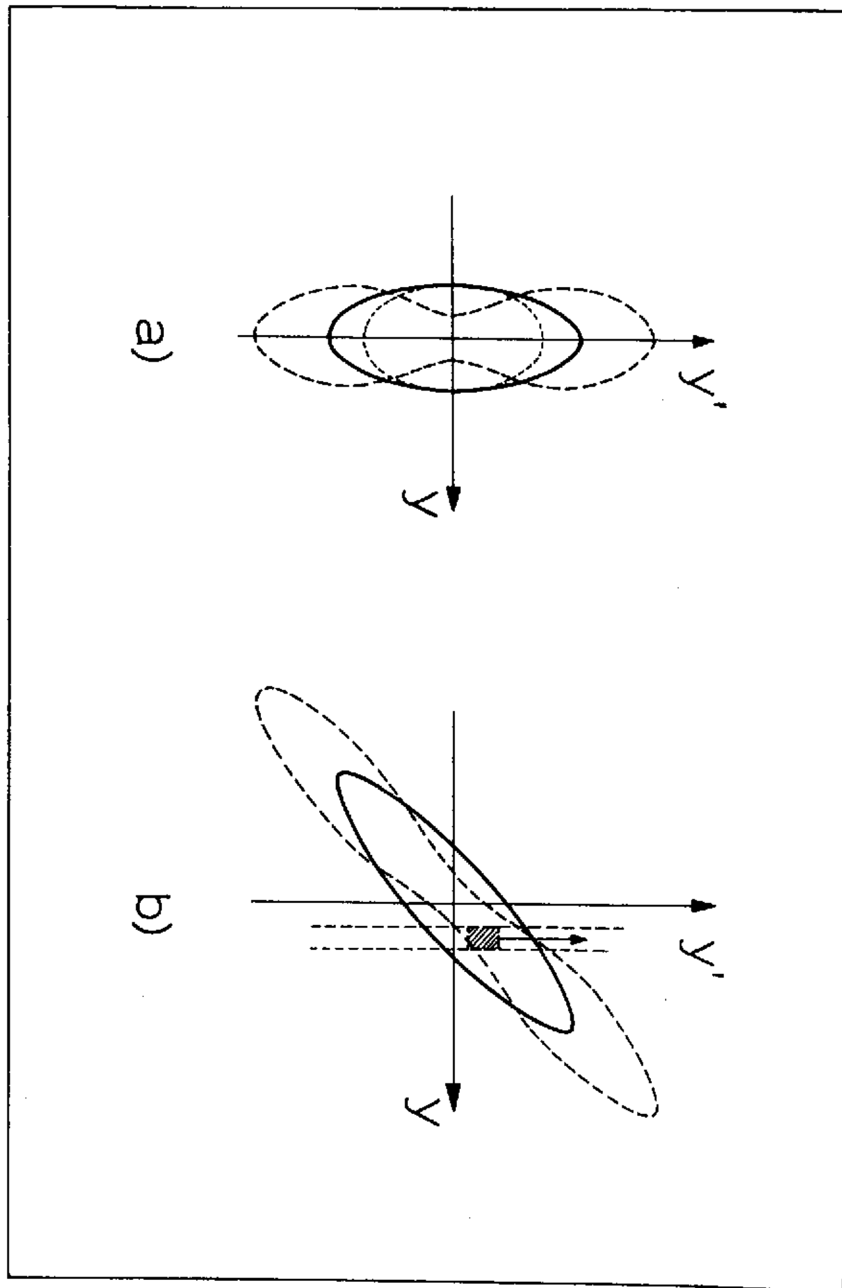

Fig. 1

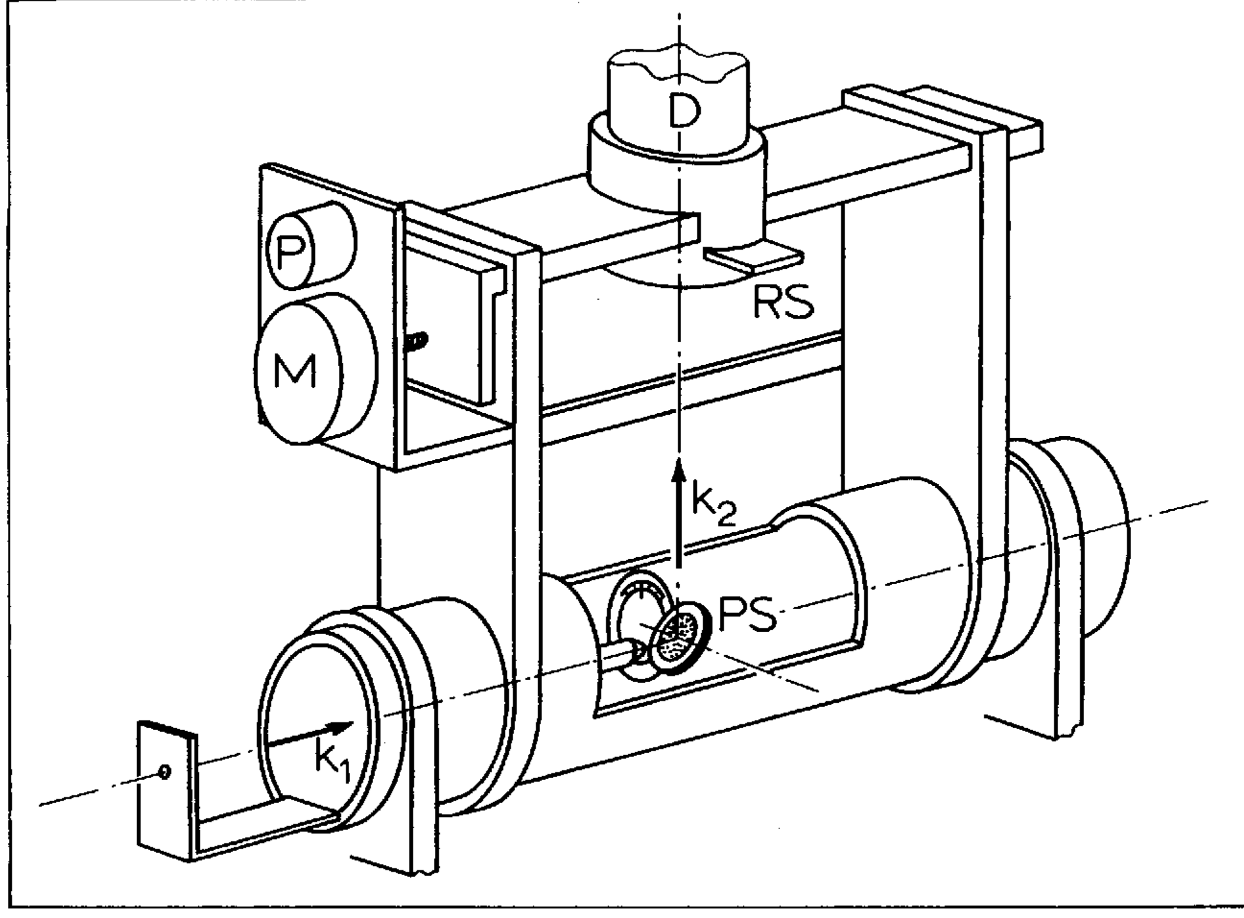

Fig. 3

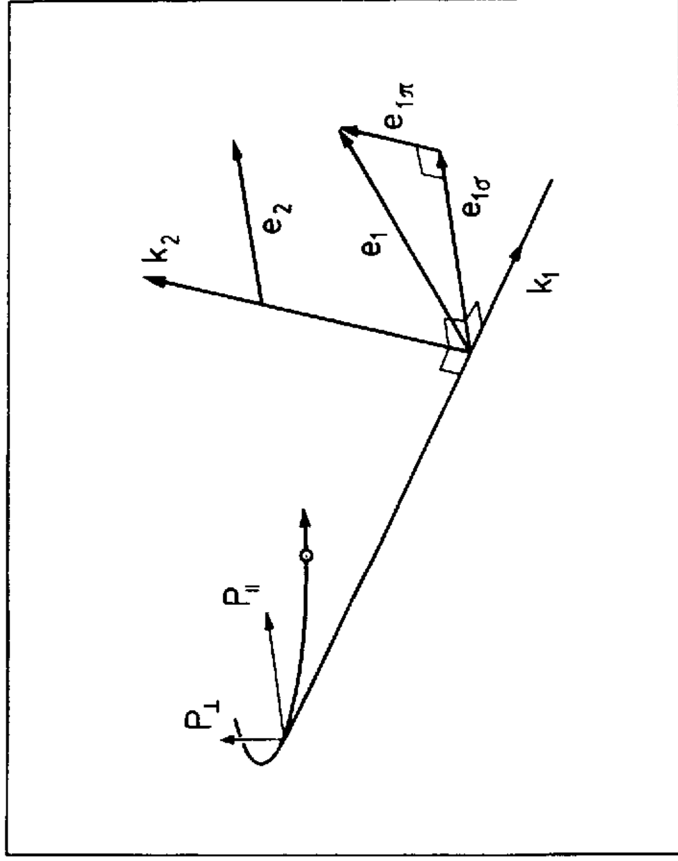

Fig. 2

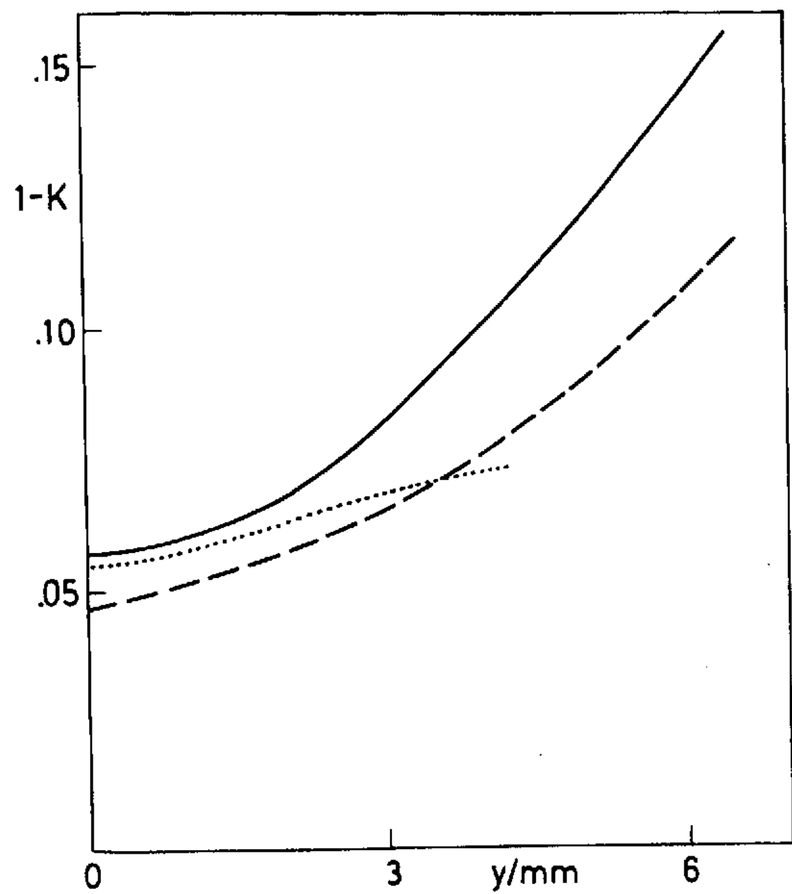

Fig. 4

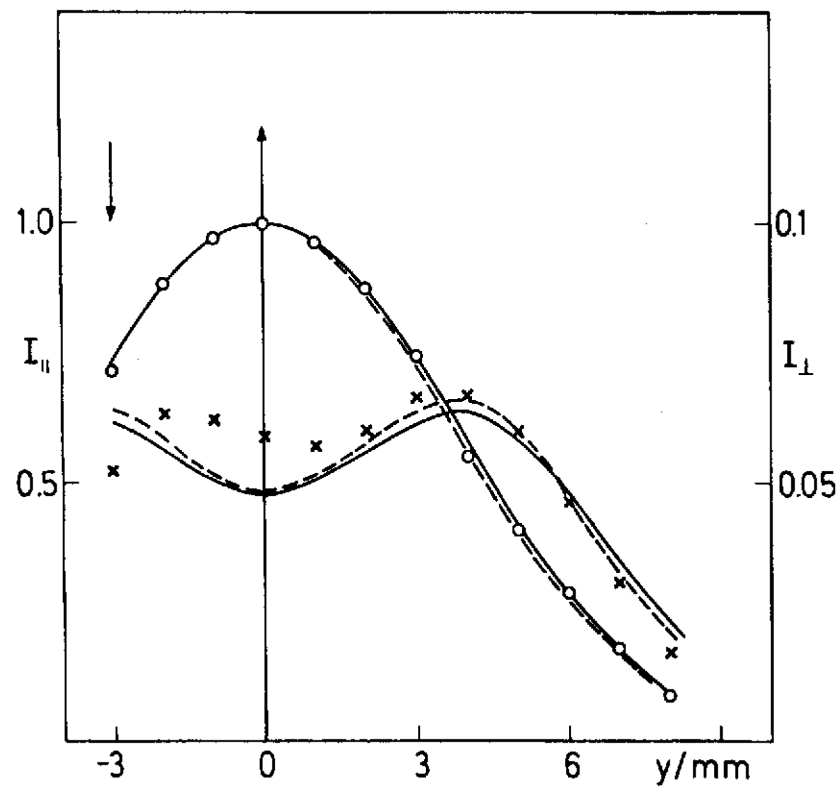

Fig. 5

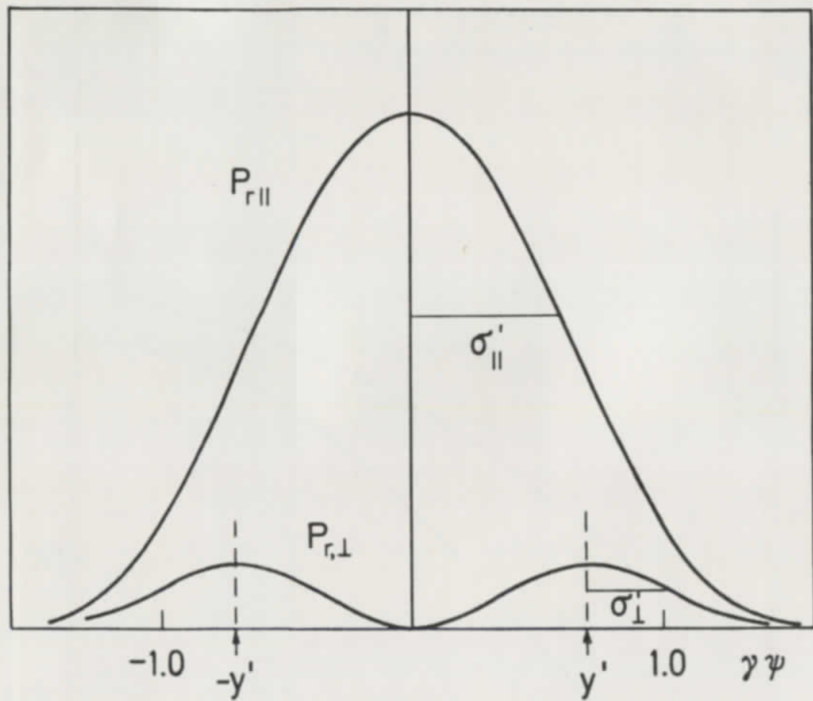

Fig. 6